Chinese Journal of Electronics
vol. 33, no. 2, pp. 564–572, March 2024
https://doi.org/10.23919/cje.2022.00.069

RESEARCH ARTICLE

Performance Study of MIMO-OSTBC Parallel Relay FSO System Based on GFDM

Rui ZHOU[2], Yong WANG[2], and Yi WANG[1,2]

1. *State Key Laboratory of Hydrology-Water Resources and Hydraulic Engineering, Hohai University, Nanjing 210098, China*
2. *Key Laboratory of Electromagnetic Wave Information Technology and Metrology of Zhejiang Province, College of Information Engineering, China Jiliang University, Hangzhou 310018, China*

Corresponding author: Yi WANG, Email: wcy16@cjlu.edu.cn
Manuscript Received April 1, 2022; Accepted April 26, 2023

Abstract — This paper investigates the performance of a new generalized frequency division multiplexing (GFDM) parallel relay free space optical (FSO) communication system using multi-input multi-output (MIMO) orthogonal space-time block codes (OSTBC) scheme. Under the M distribution atmospheric turbulence, taking into account the triple effects of irradiance, pointing errors and path loss, the mathematical expression of system symbol error rate is derived with the help of Meijer G-function. The symbol error performance of GFDM is compared with on-off keying, Gaussian minimum shift keying, polarization shift keying and orthogonal frequency division multiplexing (OFDM) modulation methods. The effects of the MIMO-OSTBC parallel relay scheme on the GFDM system including filter roll down coefficient, the number of transmitting and receiving antennas, the number of relays, normalized beamwidth and jitter variance are analyzed, and the numerical results are verified by Monte Carlo simulation. This work provides a good foundation for engineering applications.
Keywords — Free-space optical, Generalized frequency division multiplexing, Multi-input multi-output, Orthogonal space-time block codes, Parallel relay.
Citation — Rui ZHOU, Yong WANG, and Yi WANG, "Performance Study of MIMO-OSTBC Parallel Relay FSO System Based on GFDM," *Chinese Journal of Electronics*, vol. 33, no. 2, pp. 564–572, 2024. doi: 10.23919/cje.2022.00.069.

I. Introduction

Free-space optical (FSO) communication technology is based on atmospheric transmission and laser modulation [1]. It is widely used in metropolitan area network expansion, cellular backhaul networks [2], and confidential military communication and other fields, thanks to its advantages such as large communication capacity, high confidentiality, and unlicensed frequency spectrum usage [3]. However, the atmospheric turbulence encountered by the laser beam on the propagation path, and the pointing errors between communication platforms will cause the optical signal to flicker and undergo distortion in amplitude and phase. Consequently, the communication performance of the FSO system will be greatly degraded, and the system efficiency will also be reduced due to the characteristics of point-to-point transmission. In order to effectively resist the influence of atmospheric turbulence on the FSO and reduce the loss of the communication system, the combination of modulation and diversity technology has become an important means in the field of FSO communication.

Currently, different modulation techniques have been widely studied in the FSO field, such as on-off keying (OOK) [4], [5], Gaussian minimum shift keying (GMSK) [6], polarization shift keying (PolSK) [7], and orthogonal frequency division multiplexing (OFDM). Among these modulations, OFDM has been widely used in 4G scenarios. It is a typical multicarrier modulation technology that can support flexible frequency selective scheduling and effectively combat multipath fading [8]–[10]. For example, in [9], the performance of LDPC coded MIMO-OFDM communication scheme was studied, and the average bit error rate (BER) and diversity throughput of the system were analyzed. In [10], OFDM was applied to the serial-parallel combined relay FSO system, and the conclusion

Associate Editor: Prof. Yaxin ZHANG, University of Electronic Science and Technology of China.

was that this system has shown great superiority compared with the traditional FSO communication scheme. However, its spectrum efficiency is low due to problems such as high out-of-band (OOB) emission, cyclic prefix (CP) redundancy and high peak-to-average power ratio (PAPR), which can no longer meet the requirements of future mobile communication [11].

In this context, general frequency division multiplexing (GFDM) has shown great advantages and has become one of the competitive alternatives in 5G communications. It transmits through independent data blocks, and each block contains several subcarriers and subsymbols. By configuring the number of subcarriers and subsymbols in different scenarios, it has a flexible frame structure and can be applied to different service types [12], [13].

Compared with OFDM, GFDM has overcome some difficulties while retaining the main advantages of OFDM. For example, in traditional OFDM modulation, one symbol requires one CP, while in GFDM, only a single CP can be used in a frame containing multiple subsymbols, which ensures minimal overhead [14]. Therefore, GFDM has a greater advantage over OFDM in terms of spectrum efficiency. Then, GFDM is a non-orthogonal multicarrier transmission technology, which can resist frequency offset and phase noise very well. Therefore, GFDM has less requirements for synchronization process than OFDM. In addition, the choice of pulse shaping filter in the GFDM system is very flexible, which further adds a degree of freedom to GFDM. And GFDM performs pulse shaping on each subcarrier, so it can effectively suppress OOB radiation and PAPR and is suitable for combining with opportunistic access technologies to improve the spectrum utilization of fragmented white space. It is one of the main modulation technologies that can meet the large-capacity and ultra-high-speed 5G communication requirements [14]–[16]. At present, there is very limited research on its application in the field of FSO.

A multi-input multi-output (MIMO) system forms multiple channels between transceivers to combat channel fading, while orthogonal space-time block codes (OSTBC) technology can combine the spatial and time domains to improve information transmission performance without increasing bandwidth and transmission power. The OSTBC scheme can not only implement simple encoding and decoding, it can also simultaneously provide full diversity. Bhatnagar *et al.* studied the BER and system capacity of the Alamouti STBC coding system using MPSK modulation under the gamma-gamma atmospheric turbulence channels [17]. In [18], Yi *et al.* paid attention to the symbol error performance of the OSTBC transmission method under double generalized gamma fading model. The results indicated that using the OSTBC method can effectively improve system performance. However, their work only considered the direct transmission link between the transmitter and receiver, and did not introduce a relay system. The relay technology includes serial and parallel relays, where the latter can use distributed transmission mode to obtain spatial diversity gain. At present, to the best of our knowledge, the research of introducing MIMO-OSTBC into the parallel relay-assisted FSO system is very limited.

Motivated by the aforementioned literature review, this paper proposes a MIMO-OSTBC parallel relay FSO communication system using GFDM modulation over M distribution channels, which effectively alleviates the channel fading caused by atmospheric turbulence and enhances the symbol error performance of the system. Taking into account the influence of pointing errors and path loss, the closed-form expression of the average symbol error rate (SER) of the system is derived with the help of the Meijer G-function. In the proposed system, the SER of general frequency division multiplexing and other different modulations are compared, and the influence of the filter roll-off factor, the number of transceiver antennas, the number of relays, the normalized beamwidth and jitter on MIMO-OSTBC parallel relay GFDM system are analyzed.

II. Channel Attenuation Model

The joint channel attenuation effect of the atmospheric channel in the FSO system can be expressed as $h = h_a h_l h_p$ where h_a is the attenuation caused by the irradiance scintillation, h_l is the path loss, and h_p represents the pointing errors due to the misalignment between the transmitter and the receiver.

1. Path loss

The path loss is introduced by the propagation environment between the transmitter and the receiver and obeys the Lambert-Beer law. It can be written as follows [19]:

$$h_l(z) = \exp(-\sigma z) \tag{1}$$

where z is the transmission distance of the optical signal, and σ is the attenuation coefficient. Generally, path loss is a constant.

2. Pointing errors

For long-distance wireless optical communication links, the fixed transmitter and receiver platforms will be affected by phenomena such as wind load, jitter, thermal expansion and contraction in the external environment, resulting in random swings. Therefore, the power of the received optical signal is reduced, which affects the performance of the communication link. The probability density function (PDF) of pointing errors can be obtained as [20]

$$f_{h_p}(h_p) = \frac{g^2}{A_0^{g^2}}(h_p)^{g^2-1}, \quad 0 \le h_p \le A_0 \tag{2}$$

where the part of the collected power at the radial distance $\tau = 0$ is represented by $A_0 = [\mathrm{erf}(\nu)]^2$, $\mathrm{erf}(\cdot)$ denotes

the complementary error function, $\nu = \sqrt{\pi}r/2w_z$, w_z represents the beamwidth, and r represents the radius of the incident wave cross section. The ratio between the equivalent beam radius w_{zeq} at the receiving end and the pointing error jitter offset δ_s is given by g, in which

$$w_{\text{zeq}} = \left[w_z^2\sqrt{\pi}\text{erf}\left(\nu\right)/2\nu\exp\left(-\nu^2\right)\right]^{1/2}$$

The normalized beamwidth and jitter are represented by w_z/r and δ_s/r, respectively.

3. Atmospheric turbulence

In FSO communication, atmospheric turbulence has serious interference to the performance of transmission system. The laser transmitted in turbulence will cause the phase and intensity fluctuation of the beam, which greatly affect the transmission rate and accuracy. M distribution can simulate all the atmospheric turbulence channel conditions of weak, moderate and strong. It covers most of the existing statistical models of irradiance fluctuation and fit with experimental data.

The PDF of M distribution irradiance is expressed as follows [21]:

$$f_{h_a}\left(h_a\right) = A\sum_{k=1}^{\beta} a_k h_a^{\frac{\alpha+k-1}{2}} K_{\alpha-k}\left(2\sqrt{\frac{\alpha\beta h_a}{\xi\beta+\Omega'}}\right) \tag{3}$$

where

$$\begin{cases} A = \dfrac{2\alpha^{\alpha/2}}{\xi^{1+\alpha/2}\Gamma\left(\alpha\right)}\left(\dfrac{\xi\beta}{\xi\beta+\Omega'}\right)^{\beta+\alpha/2} \\ a_k = \begin{pmatrix} \beta-1 \\ k-1 \end{pmatrix}\dfrac{\left(\xi\beta+\Omega'\right)^{1-k/2}}{(k-1)!}\left(\dfrac{\Omega'}{\xi}\right)^{k-1}\left(\dfrac{\alpha}{\beta}\right)^{k/2} \end{cases} \tag{4}$$

where α represents the effective number of large-scale units in scattering environments, natural number β is related to the diffraction effect produced by small-scale eddy currents, and $K_v\left(\cdot\right)$ represents the modified Bessel function of order ν. The average power of the classical scattering component is given by $\xi = 2b_0\left(1-\rho\right)$, where ρ $(0 \le \rho \le 1)$ denotes the ratio between the scattered power coupled with the line of sight (LOS) and the power of all scattered components. The parameter Ω' represents the contribution of the coherent average power, and $\Gamma\left(\cdot\right)$ is the gamma function.

4. Joint channel attenuation model

Under the joint atmospheric channel state, the PDF of the attenuation is expressed as [22]

$$f_h\left(h\right) = \int f_{h|h_a}\left(h|h_a\right) f_{h_a}\left(h_a\right)\mathrm{d}h_a \tag{5}$$

where $f_{h|h_a}\left(h|h_a\right)$ is the conditional probability when atmospheric attenuation exists, and it can be calculated as follows:

$$\begin{aligned} f_{h|h_a}\left(h|h_a\right) &= \frac{1}{h_a h_l} f_{h_p}\left(\frac{h}{h_a h_l}\right) \\ &= \frac{g^2}{A_0^{g^2} h_a h_l}\left(\frac{h}{h_a h_l}\right)^{g^2-1}, \\ &\quad 0 \le h \le A_0 h_a h_l \end{aligned} \tag{6}$$

According to (3), (5), (6), the PDF under the joint attenuation channel can be obtained:

$$\begin{aligned} f_h\left(h\right) =& \frac{Ag^2}{2h}\sum_{k=1}^{\beta} a_k\left(\frac{\alpha\beta}{\xi\beta+\Omega'}\right)^{-\frac{\alpha+k}{2}} \\ &\times G_{1,3}^{3,0}\left[\frac{\alpha\beta h}{\left(\xi\beta+\Omega'\right)A_0 h_l}\middle|\begin{matrix}1+g^2 \\ g^2,\alpha,k\end{matrix}\right] \end{aligned} \tag{7}$$

where $G\left(\cdot\right)$ represents the Meijer G-function [23].

III. System Model

In Figure 1(a), a parallel relay MIMO transmission scheme is shown, which is a two-hop system composed of a source node S, a destination node D as well as W decode-and-forward (DF) relays. Each relay is equipped with an optical transmitter Tx and an optical receiver Rx. It is assumed that the source node and the transmitting end of each of the W relays use the same OSTBC scheme and have N_t transmitting antennas, and the receiving end of each relay and destination node have N_r receiving antennas.

The system uses GFDM-QPSK modulation, and its OSTBC transmission process is shown in Figure 1(b). In the transmitter, the input signal is first converted into a

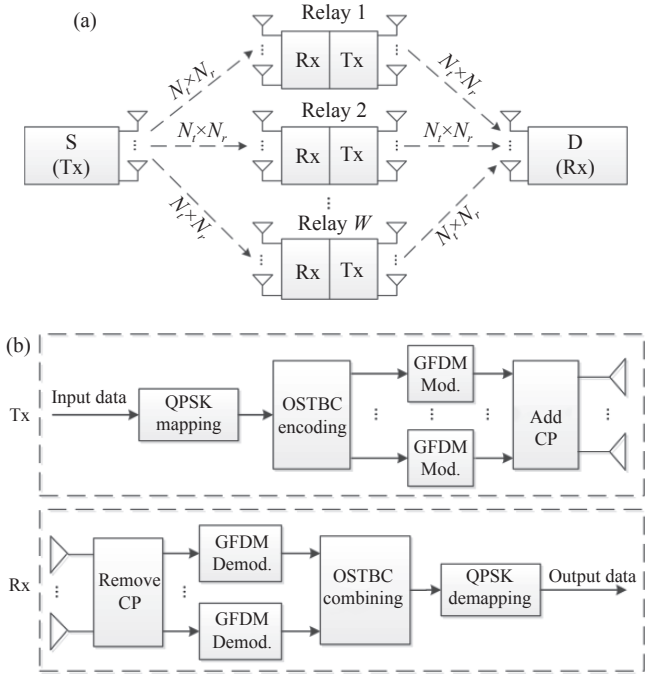

Figure 1 System model. (a) Parallel relay MIMO-OSTBC system model based on GFDM modulation. (b) GFDM MIMO-OSTBC system model. (Tx: transmitter, Rx: receiver).

complex form by a QPSK mapper. The mapped signal is then passed through an OSTBC encoder followed by GFDM modulation and the addition of CP. The final signal is then transmitted from the corresponding antenna to the FSO channels.

On the other hand, at the receiver, the optical signal is detected and then processed in reverse. For the parallel relay communication method, the total performance of the system can be obtained from the performance of each single hop in each path. Therefore, only the jth parallel path of the ith hop is considered when the transmission model is established, where $i = 1, 2$; $j = 1, 2, \ldots, W$. In the FSO system, assuming that the data symbols are transmitted through T time slots, the general form of the transmission matrix under the OSTBC scheme is as follows [24]:

$$\boldsymbol{X} = \begin{bmatrix} x_{11} & x_{21} & \cdots & x_{N_t 1} \\ x_{12} & x_{22} & \cdots & x_{N_t 2} \\ \cdots & \cdots & \ddots & \cdots \\ x_{1T} & x_{2T} & \cdots & x_{N_t T} \end{bmatrix} \tag{8}$$

where x_{mt} represents the constellation component of the signal transmitted from the mth transmitting antenna in the tth slot, $t = 1, 2, \ldots, T$. Then the transmission model is expressed as

$$\boldsymbol{Y} = \frac{\eta}{N_t}\boldsymbol{H}\boldsymbol{X} + \boldsymbol{Z} \tag{9}$$

where η is the photodetector responsivity, $\boldsymbol{H}$ represents the independent and identically distributed channel coefficient matrix of M distribution in the ith hop and jth path, and $\boldsymbol{Z}$ denotes the additive white Gaussian noise (AWGN) matrix with zero mean and variance of $N_0/2$. In the ideal channel state, after decoding at the receiver, equation (9) can be rewritten as follows:

$$\boldsymbol{y} = \frac{\eta}{N_t}\|\boldsymbol{H}\|_F^2 \boldsymbol{x} + \boldsymbol{z} \tag{10}$$

where $\boldsymbol{y}$ represents the complex matrix after decoding, $\boldsymbol{x}$ and $\boldsymbol{z}$ represents the input matrix and AWGN matrix, respectively. The square of the Frobenius norm of $\boldsymbol{H}$ is represented by $\|\boldsymbol{H}\|_{\mathrm{F}}^2 = \sum_m^{N_t}\sum_n^{N_r} h_{mn}^2$, where h_{mn} is the channel attenuation factor between the mth transmitting and nth receiving antennas, with $m = 1, 2, \ldots, N_t$; $n = 1, 2, \ldots, N_r$. Hence, in the OSTBC scheme, the instantaneous signal-to-noise ratio (SNR) is expressed as

$$\gamma_{\mathrm{OSTBC}} = \frac{\overline{\gamma}}{{N_t}^2}\|\boldsymbol{H}\|_{\mathrm{F}}^2 = \frac{\overline{\gamma}}{{N_t}^2}\sum_{m=1}^{N_t}\sum_{n=1}^{N_r} h_{mn}^2 \tag{11}$$

where the equivalent SNR $\overline{\gamma}$ can be expressed in the GFDM system as [14]

$$\overline{\gamma} = \frac{3R_T}{2(M-1)\zeta}\gamma_{av} \tag{12}$$

where M and γ_{av} represent the mapping order and the average SNR, respectively. ζ is the noise enhancement factor and is related to the receiver type and the filter roll-off factor. R_T can be defined as

$$R_T = \frac{\Theta}{\Theta + N_{cp} + N_{cs}} \tag{13}$$

where $\Theta = SK$, S and K respectively denote the number of subcarriers and subsymbols in GFDM modulation, N_{cp} and N_{cs} represent the lengths of the CP and cyclic suffix (CS), respectively.

IV. Average SER Performance Analysis

The SER represents the data transmission accuracy within a specified time. The conditional SER of the GFDM system with the QPSK mapping method can be obtained as follows:

$$P_s = 2Q\left(\sqrt{\gamma_{av}h^2\frac{3R_T}{(M-1)\zeta}}\right) \tag{14}$$

Then, according to equations (12)–(14), the SER of the jth parallel path of the ith hop for the OSTBC transmission scheme under the M distributed atmospheric turbulence joint channel is written as

$$P_{s,AV,ij} = \int_{\boldsymbol{h}} f_h(\boldsymbol{h}) \cdot 2Q\left(\sqrt{\frac{3R_T\gamma_{av}}{(M-1)\zeta N_t^2}\sum_{m=1}^{N_t}\sum_{n=1}^{N_r} h_{mn}^2}\right)\mathrm{d}\boldsymbol{h} \tag{15}$$

where $f_h(\boldsymbol{h})$ refers to the joint PDF of the vector $\boldsymbol{h} = (h_{11}, h_{12}, \ldots, h_{N_tN_r})$ that has a length equal to $N_t \times N_r$, and $Q(\cdot)$ represents the Gaussian Q-function.

Using $Q(x) \approx (1/12)\exp(-x^2/2) + (1/4)\exp(-2x^2/3)$ and $\exp(-x) = G_{0,1}^{1,0}\left[x\,\middle|_0^-\right]$, equation (15) can be rewritten as follows:

$$P_{S,AV,ij} = \frac{1}{6}\prod_{m=1}^{N_t}\prod_{n=1}^{N_r}\int_0^{\infty} f_{h_{mn}}(h_{mn}) G_{0,1}^{1,0}\left[\frac{3R_T\gamma_{av}}{2(M-1)\zeta N_t^2}h_{mn}^2\,\middle|_0^-\right]\mathrm{d}h_{mn} + \frac{1}{2}\prod_{m=1}^{N_t}\prod_{n=1}^{N_r}\int_0^{\infty} f_{h_{mn}}(h_{mn}) G_{0,1}^{1,0}\left[\frac{2R_T\gamma_{av}}{(M-1)\zeta N_t^2}h_{mn}^2\,\middle|_0^-\right]\mathrm{d}h_{mn} \tag{16}$$

Based on (7) and (16), the SER of the jth parallel path of the ith hop of the system is calculated by (17). The total average SER of the GFDM double-hop parallel relay structure using DF relay transmission mode depends

on the average SER of each relay. Hence, the total average SER of system can be expressed as (18). Then, the average SER of the GFDM parallel relay system under OSTBC transmission scheme can be calculated by (19).

$$\begin{aligned}P_{S,AV,ij}=&\frac{1}{6}\prod_{m=1}^{N_t}\prod_{n=1}^{N_r}\frac{Ag^2}{\pi}\sum\nolimits_{k=1}^{\beta}a_k\cdot 2^{\alpha+k-4}\left(\frac{\alpha\beta}{\xi\beta+\Omega'}\right)^{\frac{-\alpha-k}{2}}\\&\times G_{6,3}^{1,6}\left[\frac{24R_T\gamma_{av}(A_0h_l)^2}{(M-1)\,\zeta{N_t}^2}\left(\frac{\alpha\beta}{\xi\beta+\Omega'}\right)^{-2}\middle|\begin{matrix}\frac{1-g^2}{2},\frac{2-g^2}{2},\frac{1-\alpha}{2},\frac{2-\alpha}{2},\frac{1-k}{2},\frac{2-k}{2}\\0,\frac{-g^2}{2},\frac{1-g^2}{2}\end{matrix}\right]\\&+\frac{1}{2}\prod_{m=1}^{N_t}\prod_{n=1}^{N_r}\frac{Ag^2}{\pi}\sum\nolimits_{k=1}^{\beta}a_k\cdot 2^{\alpha+k-4}\left(\frac{\alpha\beta}{\xi\beta+\Omega'}\right)^{\frac{-\alpha-k}{2}}\\&\times G_{6,3}^{1,6}\left[\frac{32R_T\gamma_{av}(A_0h_l)^2}{(M-1)\zeta{N_t}^2}\left(\frac{\alpha\beta}{\xi\beta+\Omega'}\right)^{-2}\middle|\begin{matrix}\frac{1-g^2}{2},\frac{2-g^2}{2},\frac{1-\alpha}{2},\frac{2-\alpha}{2},\frac{1-k}{2},\frac{2-k}{2}\\0,\frac{-g^2}{2},\frac{1-g^2}{2}\end{matrix}\right]\end{aligned}\tag{17}$$

$$P_{s,AV}=\prod_{j=1}^{W}P_{s,j}=\prod_{j=1}^{W}\left[1-\prod_{i=1}^{2}(1-P_{s.ij})\right]=\prod_{j=1}^{W}\left[1-(1-P_{s.ij})^2\right]\tag{18}$$

$$P_{S,AV}=\prod_{j=1}^{W}\left[1-\left(1-\left(\begin{aligned}&\frac{1}{6}\prod_{m=1}^{N_t}\prod_{n=1}^{N_r}\frac{Ag^2}{\pi}\sum\nolimits_{k=1}^{\beta}a_k\left(\frac{\alpha\beta}{\xi\beta+\Omega'}\right)^{\frac{-\alpha-k}{2}}\cdot 2^{\alpha+k-4}\\&\times G_{6,3}^{1,6}\left[\frac{24R_T\gamma_{av}(A_0h_l)^2}{(M-1)\,\zeta{N_t}^2}\left(\frac{\alpha\beta}{\xi\beta+\Omega'}\right)^{-2}\middle|\begin{matrix}\frac{1-g^2}{2},\frac{2-g^2}{2},\frac{1-\alpha}{2},\frac{2-\alpha}{2},\frac{1-k}{2},\frac{2-k}{2}\\0,\frac{-g^2}{2},\frac{1-g^2}{2}\end{matrix}\right]\\&+\frac{1}{2}\prod_{m=1}^{N_t}\prod_{n=1}^{N_r}\frac{Ag^2}{\pi}\sum\nolimits_{k=1}^{\beta}a_k\left(\frac{\alpha\beta}{\xi\beta+\Omega'}\right)^{\frac{-\alpha-k}{2}}\cdot 2^{\alpha+k-4}\\&\times G_{6,3}^{1,6}\left[\frac{32R_T\gamma_{av}(A_0h_l)^2}{(M-1)\zeta{N_t}^2}\left(\frac{\alpha\beta}{\xi\beta+\Omega'}\right)^{-2}\middle|\begin{matrix}\frac{1-g^2}{2},\frac{2-g^2}{2},\frac{1-\alpha}{2},\frac{2-\alpha}{2},\frac{1-k}{2},\frac{2-k}{2}\\0,\frac{-g^2}{2},\frac{1-g^2}{2}\end{matrix}\right]\end{aligned}\right)\right)^2\right]\tag{19}$$

V. Numerical Simulation and Results

Based on the aforementioned derived formulas, this section evaluates the average SER performance based on numerical and Monte Carlo simulations. Under the M distribution joint atmospheric channels, the atmospheric refractive index structure constants are $C_n^2=2.3\times10^{-13}$ $\mathrm{m}^{-2/3}$ (strong turbulence, $\alpha=4.86$, $\beta=1$, $\sigma_R^2=4.58$) and $C_n^2=2.3\times10^{-14}$ $\mathrm{m}^{-2/3}$ (weak turbulence, $\alpha=6.30$, $\beta=5$, $\sigma_R^2=0.46$). The phase difference between the LOS and the coupled scattering is $\Phi_A-\Phi_B=\pi/2$, $(\Omega,\rho,b_0)=(0.5,0.75,0.5)$, and the laser wavelength $\lambda=1550$ nm. The link length between Tx and Rx is equal to $z=1000$ m, and the normalized beamwidth and jitter are fixed as $w_z/r=5$ and $\delta_s/r=1$, respectively. The parameters used for simulation of the GFDM signal are as follows: The number of subcarriers and subsymbols are $S=64$ and $K=5$, respectively; lengths of the CP and CS are 8 and 0, respectively; the receiving end uses a zero forced (ZF) receiver; the pulse shaping filter used by the GFDM system is an raised cosine (RC) filter; and the value of the roll-off factor is $\varepsilon=0.5$.

Figure 2 compares the average SER with the $2\subseteq3$ OSTBC scheme when the system adopts different modulation schemes under the strong and weak atmospheric turbulence, where the number of relays $W=2$. It can be seen from the figure that the numerical results are consistent with the Monte Carlo curve. As the average SNR increases, the SER of the system decreases. Among several different modulations, the GFDM system performs better than OOK, GMSK and PolSK, but worse than OFDM. This is because GFDM abandons the strict orthogonality between subcarriers, resulting in the increase of subcarrier interference. However, a communication system using GFDM modulation can obtain lower PAPR and OOB values, and higher spectrum utilization efficiency than OFDM modulation.

Figure 3 describes the average SER of the MIMO-OSTBC parallel relay GFDM system with different roll-off factor under the strong and weak turbulence. The $2\subseteq3$ OSTBC scheme is adopted, and the number of relays $W=2$. It can be seen from the figure that the smaller the roll-off factor ε, the better the SER performance of the system. This is because the smaller the ε, the higher the utilization rate of the frequency band and the lower the in-band noise. However, after matching and filtering the signal at the receiving end, the inter-symbol crosstalk will be amplified, resulting in performance degradation. When ε is increased, the oscillation of the time-domain waveform of the filter is reduced and attenuates rapidly, which is beneficial to reduce the inter-symbol crosstalk. However, this will occupy a larger fre-

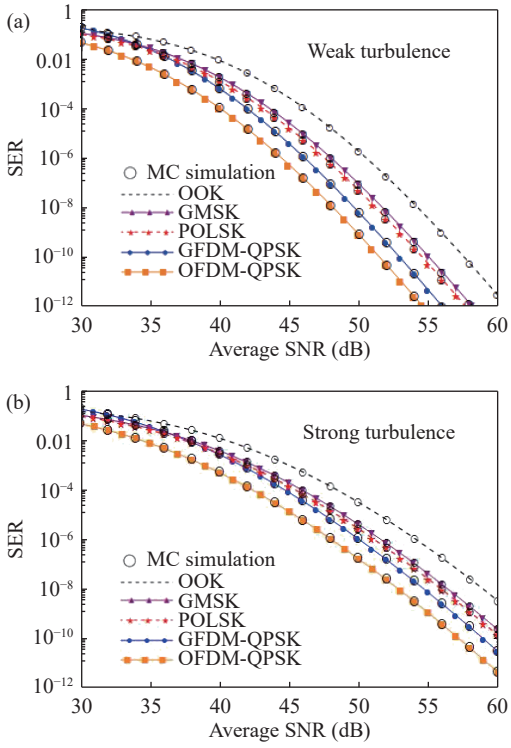

Figure 2 Average SER of MIMO-OSTBC parallel relay system with different modulation methods. (a) weak turbulence, and (b) strong turbulence.

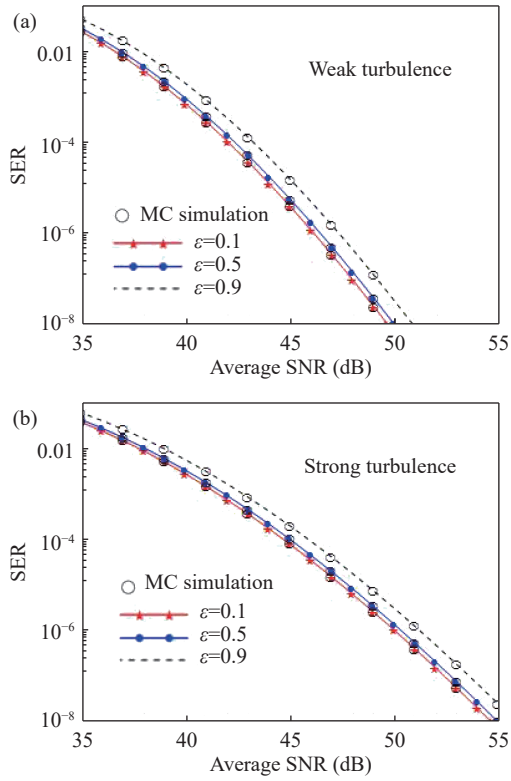

Figure 3 Average SER of MIMO-OSTBC parallel relay GFDM system with different roll-off factor. (a) Weak turbulence; (b) Strong turbulence.

quency band, resulting in lower utilization of the frequency band and higher in-band noise. Hence, the value of ε is not as small as possible, and it is more appropriate to take 0.5 in comprehensive consideration.

Figure 4 illustrates the SER curve of the MIMO-OSTBC parallel relay GFDM-QPSK FSO system under the strong and weak turbulence with the average SNR, where the number of parallel relays $W = 2$. It can be clearly seen that the Monte Carlo simulation and numerical analysis curves fit well. By increasing the average SNR, the SER of the system decreases. It can be seen from the figure that the introduction of OSTBC has significantly improved the performance of the system. In the strong turbulence communication link, if the SER of the system reaches 10^{-5} to maintain normal communication, the uncoded system needs an SNR of higher than 70 dB, which necessitates higher laser output power, leading to a significant increase in the cost of the system. On the other hand, lower SNR values of 63 dB, 47 dB and 41 dB are required by the 2×1, 2×2 and 2×3 OSTBC systems, respectively. Therefore, it can be analyzed that as the transceiver antenna increases, the SER of the system decreases and the ability to resist fading increases. The effect of space diversity gain is very obvious.

When the transmitter and receiver platforms can only be equipped with limited transceiver antennas and are unable to meet the communication requirements, it is necessary to introduce a parallel relay to obtain diversity gain. In Figure 5, the symbol error performance of the GFDM system using MIMO-OSTBC parallel relay

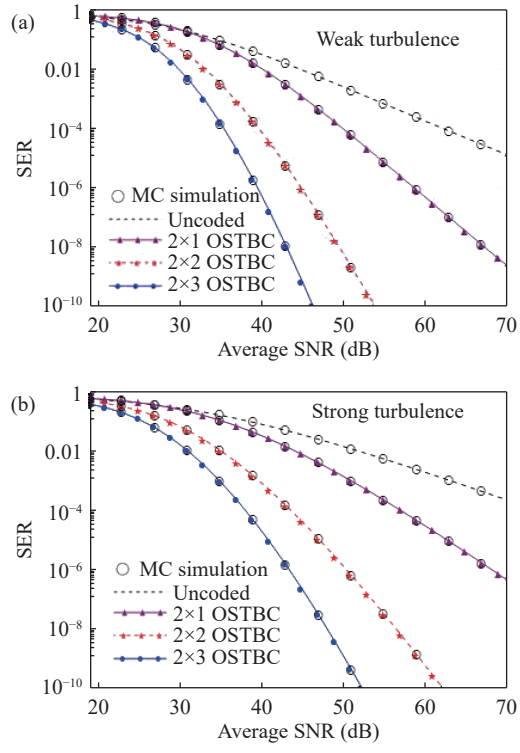

Figure 4 Average SER of MIMO-OSTBC parallel relay GFDM system with different OSTBC schemes. (a) Weak turbulence; (b) Strong turbulence.

scheme under the strong and weak atmospheric turbu-

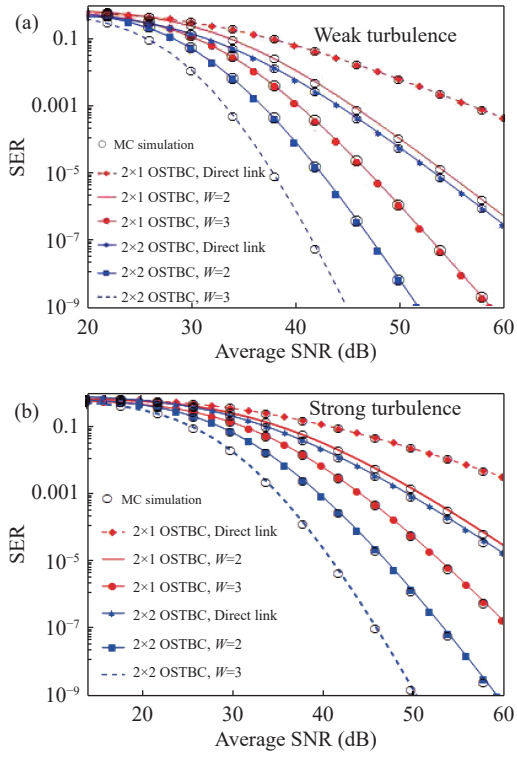

Figure 5 Average SER of MIMO-OSTBC parallel relay GFDM system with different number of relays and OSTBC schemes. (a) Weak turbulence; (b) Strong turbulence.

lence is illustrated. It can be observed from the figure that the Monte Carlo results agree with the numerical analysis. In the 2×1 OSTBC scheme, the SNR is fixed at 50 dB and the SER in the direct transmission link is 2.4×10^{-2}. On the other hand, when the numbers of relays are 2 and 3, the SER values are 1.5×10^{-3} and 6.0×10^{-5}, respectively. Hence in the MIMO-OSTBC system, increasing the number of parallel relays can effectively reduce the SER of the system in the communication process, and make the communication performance of the system increase significantly. However, this does not mean that the greater the number of relay nodes, the better the system. Taking cost into consideration, the number of relay nodes in the communication link should not be too many. The numbers of transmitting and receiving antennas and relays should be determined based on the actual scenario. From the simulation diagram, it can be observed that the system with 2×2 OSTBC scheme and $W = 3$ has the best performance, where the required SNR is only 40 dB to maintain an SER of approximately 10^{-5}.

In Figure 6, the 3D plots of the average SER of the parallel relay MIMO-OSTBC GFDM-QPSK system versus the normalized beamwidth and normalized jitter is shown. The average SNR is 25 dB and the number of relays is $W = 2$. It can be found that the SER of the system reduces as the normalized beamwidth increases, and rises as the normalized jitter increases. This behavior is obvious for a lower normalized beamwidth. In addition, by comparing Figure 6(a), 6(b) and 6(c), as the number

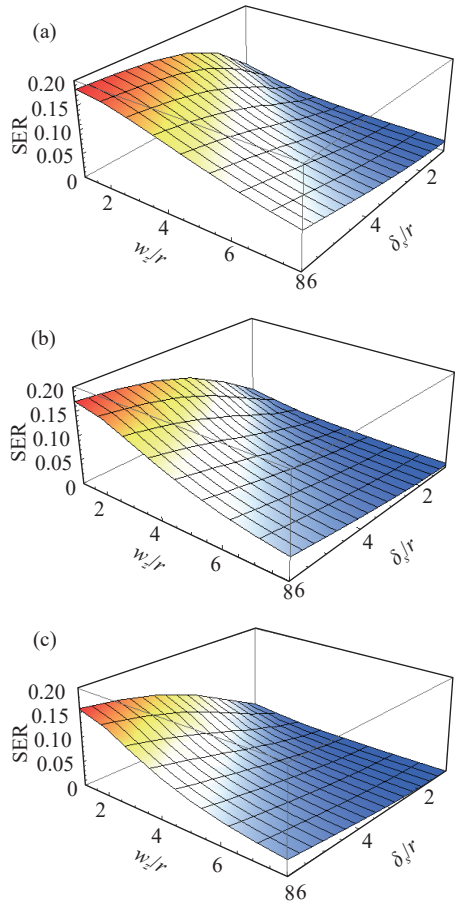

Figure 6 Average SER of parallel relay MIMO-OSTBC GFDM system versus w_z/r and δ_s/r under strong turbulence. (a) $2 \subseteq 1$ OSTBC; (b) $2 \subseteq 2$ OSTBC; (c) $2 \subseteq 3$ OSTBC.

of transceiver antennas increases, the influence of the normalized beamwidth on the system SER becomes more and more obvious, and the influence of the normalized jitter on the system SER gradually decreases. For example, when the normalized jitter is fixed at $\delta_s/r = 6$ and w_z/r is increased from 1 to 8, the SER under the 2×1, 2×2, and 2×3 OSTBC schemes are reduced by 0.102, 0.124, and 0.128, respectively. When the normalized beamwidth is set to a constant $w_z/r = 8$, and δ_s/r is reduced from 6 to 1, the SER of the system under the 2×1, 2×2, and 2×3 OSTBC schemes are reduced by 0.058, 0.039, and 0.029, respectively. Therefore, when the number of transceiver antennas is large, more attention should be paid to the beamwidth. From this we can conclude that in engineering applications, in order to control the SER within a lower range, the divergence angle of the transmitting beam can be adjusted by the laser beam expanders to achieve the optimal beamwidth and improve the communication quality of the system.

VI. Conclusions

This paper proposes a MIMO-OSTBC parallel relay FSO communication system using GFDM modulation over the M distribution atmospheric joint attenuation channels. The SER performance of the system is studied

under the triple effect of path loss, pointing errors and irradiance. The average SER expression of the system is derived, and then the theoretical results are verified by Monte Carlo method. The SERs of GFDM and other different modulations are compared in the simulation. Compared with OOK, GMSK, PolSK and OFDM modulation methods, GFDM has shown great superiority in symbol error performance, and can obtain lower PAPR and OOB value, as well as higher spectrum utilization efficiency. The influence of the roll-off factor, the number of transmitting and receiving antennas, the number of relays, the normalized beamwidth and jitter on the proposed system are illustrated. The results indicate that the larger the roll-off factor of the filter, the worse the symbol error performance of the system. Considering factors such as noise and frequency band utilization in the analysis, a value of 0.5 for ε is more appropriate. The GFDM FSO transmission system combining MIMO-OSTBC scheme and parallel relay technology has been significantly improved in terms of symbol error performance. By increasing the number of transceiver antennas and relays, the SER of the system is significantly reduced. However, considering the cost, complexity and performance improvement, the number of relays in the communication link should not be too many. The number of transceiver antennas and relays needs to be decided according to the practical application. In the simulation, the system performance with 2×2 OSTBC scheme when W of 3 is the best, and it only needs 40 dB to meet the normal communication requirements of the FSO system. In addition, increasing the normalized beamwidth and normalized jitter of the system will reduce and increase the SER, respectively. This behavior is obvious for a lower normalized beamwidth. And compared with the normalized jitter, the beamwidth has a greater impact on the SER of the system when the number of transmitting and receiving antennas is large. Therefore, in order to control the SER within a lower range, the beamwidth can be optimized by using a laser beam expander to adjust the beam divergence angle while increasing the number of transmitting and receiving antennas. Taking the above factors into consideration, the GFDM OSTBC-MIMO parallel relay system has certain guiding significance for future FSO communication systems in engineering applications.

Acknowledgement

This work was supported by the Belt and Road Special Foundation of the State Key Laboratory of Hydrology-Water Resources and Hydraulic Engineering (Grant No. 2020491411) and the National Natural Science Foundation of China (Grant No. 51704267).

References

[1] J. Poliak, P. Pezzei, P. Barcik, *et al.*, "On the derivation of exact analytical FSO link attenuation model," *Transactions on Emerging Telecommunications Technologies*, vol. 25, no. 6, pp. 609–617, 2014.

[2] X. Chen, W. C. Lyu, Z. J. Zhang, *et al.*, "56-m/3.31-Gbps underwater wireless optical communication employing Nyquist single carrier frequency domain equalization with noise prediction," *Optics Express*, vol. 28, no. 16, pp. 23784–23795, 2020.

[3] M. K. Miao and X. F. Li, "Novel approximate distribution of the sum of Gamma-Gamma variates with pointing errors and applications in MIMO FSO links," *Optics Communications*, vol. 486, article no. 126780, 2021.

[4] W. Gappmair, S. Hranilovic, and E. Leitgeb, "OOK performance for terrestrial FSO links in turbulent atmosphere with pointing errors modeled by Hoyt distributions," *IEEE Communications Letters*, vol. 15, no. 8, pp. 875–877, 2011.

[5] J. F. Feng and X. H. Zhao, "Performance analysis of OOK-based FSO systems in Gamma-Gamma turbulence with imprecise channel models," *Optics Communications*, vol. 402, pp. 340–348, 2017.

[6] D. Sarkar and S. K. Metya, "Effects of atmospheric weather and turbulence in MSK based FSO communication system for last mile users," *Telecommunication Systems*, vol. 73, no. 1, pp. 87–93, 2020.

[7] K. Prabu, S. Cheepalli, and D. S. Kumar, "Analysis of PolSK based FSO system using wavelength and time diversity over strong atmospheric turbulence with pointing errors," *Optics Communications*, vol. 324, pp. 318–323, 2014.

[8] J. Xu, Y. H. Song, X. Y. Yu, *et al.*, "Underwater wireless transmission of high-speed QAM-OFDM signals using a compact red-light laser," *Optics Express*, vol. 24, no. 8, pp. 8097–8109, 2016.

[9] M. Sharma, D. Chadha, and V. Chandra, "Performance analysis of MIMO–OFDM free space optical communication system with low-density parity-check code," *Photonic Network Communications*, vol. 32, no. 1, pp. 104–114, 2016.

[10] Y. Wang and H. Wu, "Performance study of serial-parallel combined relay orthogonal frequency division multiplexing free space optical system based on M distribution model," *Optical Engineering*, vol. 58, no. 10, article no. 106101, 2019.

[11] M. Maraş, E. N. Ayvaz, M. Cömeç, *et al.*, "A novel GFDM waveform design based on cascaded WHT-LWT transform for the beyond 5G wireless communications," *Sensors*, vol. 21, no. 5, article no. 1831, 2021.

[12] S. K. Bandari, V. V. Mani, and A. Drosopoulos, "Performance analysis of GFDM in various fading channels," *COMPEL-The International Journal for Computation and Mathematics in Electrical and Electronic Engineering*, vol. 35, no. 1, pp. 225–244, 2016.

[13] S. K. Bandari, V. M. Vakamulla, and A. Drosopoulos, "GFDM/OQAM performance analysis under Nakagami fading channels," *Physical Communication*, vol. 26, pp. 162–169, 2018.

[14] N. Michailow, M. Matthé, I. S. Gaspar, *et al.*, "Generalized frequency division multiplexing for 5th generation cellular networks," *IEEE Transactions on Communications*, vol. 62, no. 9, pp. 3045–3061, 2014.

[15] N. Michailow and G. Fettweis, "Low peak-to-average power ratio for next generation cellular systems with generalized frequency division multiplexing," in *2013 International Symposium on Intelligent Signal Processing and Communication Systems*, Naha, Japan, pp.651–655, 2013.

[16] D. Rakhimov, S. P. Deram, B. Sokal, *et al.*, "Iterative tensor receiver for MIMO-GFDM systems", in *2020 IEEE 11th Sen-*

sor Array and Multichannel Signal Processing Workshop (SAM), Hangzhou, China, pp.1–5, 2020.

[17] M. R. Bhatnagar and S. Anees, "On the performance of Alamouti scheme in Gamma-Gamma fading FSO links with pointing errors," *IEEE Wireless Communications Letters*, vol. 4, no. 1, pp. 94–97, 2015.

[18] X. Yi, M. W. Yao, and X. Y. Wang, "MIMO FSO communication using subcarrier intensity modulation over double generalized gamma fading," *Optics Communications*, vol. 382, pp. 64–72, 2017.

[19] K. A. Balaji and K. Prabu, "Performance evaluation of FSO system using wavelength and time diversity over Malaga turbulence channel with pointing errors," *Optics Communications*, vol. 410, pp. 643–651, 2018.

[20] H. G. Sandalidis, T. A. Tsiftsis, G. K. Karagiannidis, *et al.*, "BER performance of FSO links over strong atmospheric turbulence channels with pointing errors," *IEEE Communications Letters*, vol. 12, no. 1, pp. 44–46, 2008.

[21] I. S. Ansari, F. Yilmaz, and M. S. Alouini, "Performance analysis of free-space optical links over Málaga (M) turbulence channels with pointing errors," *IEEE Transactions on Wireless Communications*, vol. 15, no. 1, pp. 91–102, 2016.

[22] A. A. Farid and S. Hranilovic, "Outage capacity optimization for free-space optical links with pointing errors," *Journal of Lightwave Technology*, vol. 25, no. 7, pp. 1702–1710, 2007.

[23] Wolfram Function Site, Available at: http://functions.wolfram.com/.

[24] W. Li, H. Zhang, and T. A. Gulliver, "Capacity and error probability analysis of orthogonal space-time block codes over correlated nakagami fading channels," *IEEE Transactions on Wireless Communications*, vol. 5, no. 9, pp. 2408–2412, 2006.

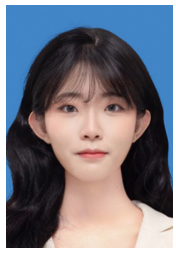

Rui ZHOU received the B.E. degree in electronic information engineering from Hengyang Normal University. She is studying for the M.S. degree at China Jiliang University. Her research interests include free-space optical communication and optical coherent detection. (Email: p20030854050@cjlu.edu.cn)

Yong WANG is studying for the M.S. degree at China Jiliang University. His research interests include secrecy performance analysis of mixed radio frequency/free-space optical communication system.
(Email: 1391662057@qq.com)

Yi WANG received the Ph.D. degree from Harbin Engineering University, Harbin, China. Currently, she is a Postdoctoral Fellow at the School of Astronautics of Harbin Institute of Technology and a Professor at China Jiliang University. Her research interests include satellite-to-ground laser communication, free-space optical communication, laser beam propagation in atmospheric turbulence, and optical coherent detection. (Email: wcy16@cjlu.edu.cn)